The Crystal Structure of $Fe_3(CO)_{11}P(C_6H_5)_3$[1]

Donald J. Dahm and Robert A. Jacobson

Contribution from the Institute for Atomic Research and Department of Chemistry, Iowa State University, Ames, Iowa 50010. *Received January 17, 1968*

Abstract: The crystal structure of $Fe_3(CO)_{11}P(C_6H_5)_3$ has been determined from three-dimensional X-ray data. Sixteen molecules crystallize in the monoclinic space group $C_{2/c}$ with $a = 37.14$, $b = 12.26$, $c = 26.05$ Å, and $\beta = 93.96°$. The structure was refined by full-matrix least squares with iron and phosphorus atoms anisotropic to a conventional R value of 0.082 for 1800 reflections collected by counter methods. The structure is similar to that of $Fe_3(CO)_{12}$. The iron atoms form a nearly isosceles triangle with the short side connected by two asymmetric carbonyl bridges. The rest of the carbonyls are terminal. Each asymmetric unit contains two molecules which are structural isomers of one another, with the $P(C_6H_5)_3$ group attached to different iron atoms.

For several years a controversy has existed concerning the molecular structure of $Fe_3(CO)_{12}$. An early X-ray crystal structure investigation[2] indicated a disordered structure, with the iron atoms forming an equilateral triangle. However, Mössbauer studies showed that two of the iron atoms had a different electronic environment than the third, and some workers interpreted this as being consistent only with a more linear model.[3-5] Subsequently a different arrangement of the carbonyls was proposed (Figure 1a) based on the crystal structure determination[6] of $HFe_3(CO)_{11}^-$ which could explain this disparity. Mössbauer data indicated that $Fe_3(CO)_{12}$ and $HFe_3(CO)_{11}^-$ have similar structures.[7] However, $HFe(CO)_{11}^-$ is not a derivative of $Fe_3(CO)_{12}$ and the two have somewhat different physical properties. Therefore, it is difficult to assess the degree of disparity between the two structures.

A derivative of $Fe_3(CO)_{12}$, namely $Fe_3(CO)_{11}P(C_6H_5)_3$ which has properties very similar to its parent,[8] was prepared and came to our attention. We felt a structural study of this derivative might well give better evidence for the exact arrangement of the iron and carbonyl groups in $Fe_3(CO)_{12}$ than studies of its own disordered crystal, and therefore we decided to undertake such a project.

Experimental Section

$Fe_3(CO)_{11}P(C_6H_5)_3$ was prepared by Angelici and Siefert[8] by the reaction of $Fe_3(CO)_{12}$ and $P(C_6H_5)_3$. They obtained dark green, plate-like single crystals by evaporation of a pentane solution. Because these crystals were reported to decompose in the atmosphere, they were placed in thin-walled, Lindemann glass capillaries.

Preliminary precession photographs (Cu Kα) showed the unit cell to be monoclinic with systematic absences: hkl when $h + k \neq 2n$, and $h0l$ when $l \neq 2n$. These absences are consistent with either space group C_s^4-C_c or C_{2h}^6-$C_{2/c}$. The unit cell parameters at 25° are $a = 37.14 \pm 0.03$, $b = 12.26 \pm 0.01$, and $c = 26.05 \pm 0.02$ Å, and $\beta = 93.96 \pm 0.15°$. These parameters and their standard deviations were obtained by averaging several reflection positions (Mo Kα radiation, λ 0.7107 Å) whose centers were determined by left–right, top–bottom beam splitting on a previously aligned General Electric single-crystal orienter. Inasmuch as this compound is either soluble or decomposes in common solvents, the density was estimated to be approximately 1.7 ± 0.2 g/cm^3 from density measurements of similar compounds. The calculated density is 1.66 g/cm^3 based on 16 molecules per unit cell.

For data collection, a crystal having approximate dimensions $0.06 \times 0.35 \times 0.19$ mm along the a, b, and c crystal axes, respectively, was mounted such that the b axis was along the axis of the capillary and hence along the spindle axis.

Data were collected at room temperature with Zr-filtered, Mo Kα radiation, utilizing a General Electric XRD-5 X-ray unit equipped with a goniostat and scintillation counter. Within a 2θ sphere of 35°, peak heights of all reflections were checked visually on a rate meter. Beyond 35°, several reflections were spot-checked to verify that there were exceedingly few reflections in this range which could be classified as "observed." This had been expected because of the rapid fall in intensities at higher angles observed on the photographs. About 1800 reflections from two octants were found to be significantly above background; their intensities were measured using a 100-sec, θ–2θ coupled scan (1.67° in 2θ) using a take-off angle of 1°.

Individual background values were obtained from a plot of measurements of background *vs.* 2θ. Intensities were further corrected for Lorentz and polarization factors, streak due to noncharacteristic radiation, and crystal decomposition. The maximum decrease in the intensity of three periodically measured standard reflections was 16%. Errors in intensities were determined as previously described.[9]

Because of the small crystal size (0.004 mm^3) and the relatively small linear absorption coefficient (16 cm^{-1}), no corrections for lost counts, extinction, or absorption were felt necessary. Since all the recorded reflections were at rather low 2θ values, the maximum X-ray path length through the crystal was only slightly more than the intermediate crystal dimension. The intensity of the $0k0$ reflections showed little variation with respect to the rotation of the φ axis, also indicating that absorption was not significant.

Structure Determination

A Patterson function was computed from sharpened data[10] and a vector which was assumed to be an Fe–Fe vector resulting from the c-glide, a symmetry element present in both possible space groups, was located on the Harker line. A superposition employing the minimum function was then carried out and readily revealed the positions of two-thirds of the iron atoms in the unit cell; in addition the presence of a center of symmetry in the unit cell was also indicated. The latter, together with an equivalent result obtained *via* a statistical test,[11] strongly suggested that the correct space group is $C_{2/c}$ as was later confirmed by the successful refinement in this space group. Using these iron positions and the

(1) Work was performed in the Ames Laboratory of the U. S. Atomic Energy Commission. Contribution No. 2243.
(2) L. F. Dahl and R. E. Rundle, *J. Chem. Phys.*, **26**, 1751 (1957).
(3) (a) M. Kalvius, U. Zahn, P. Kienle, and H. Eicher, *Z. Naturforsch.*, **17a**, 494 (1962); (b) R. H. Herber, W. R. Kingston, and G. K. Wertheim, *Inorg. Chem.*, **2**, 153 (1963).
(4) E. Fluck, W. Kerler, and W. Neuwrith, *Angew. Chem. Intern. Ed. Engl.*, **2**, 277 (1963).
(5) G. R. Dobson and R. K. Sheline, *Inorg. Chem.*, **2**, 1313 (1963).
(6) L. F. Dahl and J. F. Blount, *ibid.*, **4**, 1373 (1965).
(7) N. E. Erickson and A. W. Fairhall, *ibid.*, **4**, 1320 (1965).
(8) R. J. Angelici and E. E. Siefert, *ibid.*, **5**, 1457 (1966).
(9) L. G. Hoard and R. A. Jacobson, *J. Chem. Soc., A*, 1203 (1966).
(10) R. A. Jacobson, J. A. Wunderlich, and W. N. Lipscomb, *Acta Cryst.*, **14**, 598 (1961).
(11) E. R. Howells, D. C. Phillips, and D. Rogers, *ibid.*, **3**, 210 (1950).

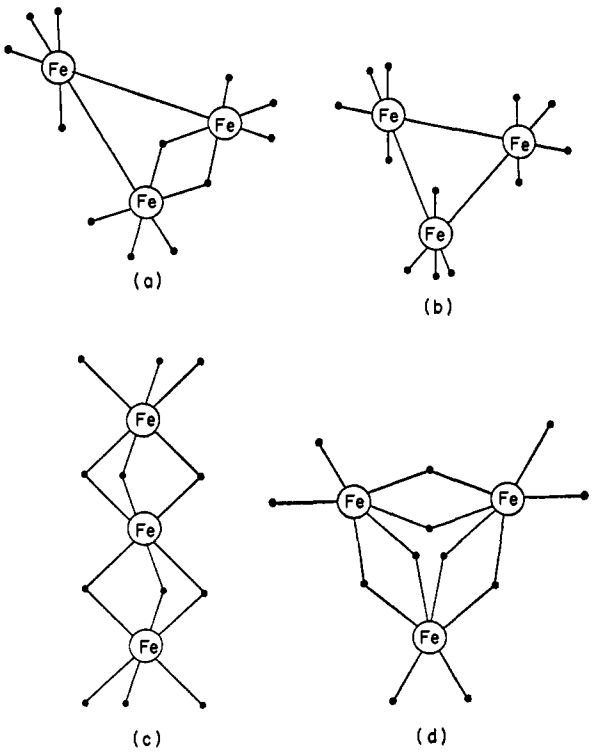

Figure 1. Proposed structures for $Fe_3(CO)_{12}$.

centric space group, the remaining atoms were found by successive structure factor and electron density map calculations.[12]

The presence of 16 molecules in a unit cell with space group of order eight requires that each asymmetric unit contain two crystallographically independent molecules. Therefore, there are 264 independent, non-hydrogen, positional parameters and the associated thermal parameters to be refined. Consequently, our first approach was to use a block-diagonal technique in an attempt to refine the structural parameters. However, satisfactory convergence did not result, probably because of the neglect of large interaction terms between adjacent atoms in this monoclinic space group. A full-matrix program was then employed, varying all the parameters of each molecule in alternating cycles. Refinement resulted in convergence with $R = \Sigma||F_o| - |F_c||/\Sigma|F_o| = 0.106$ for all atoms isotropic and $R = 0.078$ with the iron and phosphorus atoms anisotropic. The corresponding values of the weighted discrepancy factor, $wR = (\Sigma w(|F_o| - |F_c|)^2/\Sigma w(F_o)^2)^{1/2}$, are 0.131 and 0.091, respectively.

Least-squares refinement was also carried out, treating each of the six phenyl groups as a rigid group in order to reduce the number of parameters being varied. This refinement[12,13] resulted in an $R = 0.082$ and $wR = 0.097$ with the heavy atoms again anisotropic. A final difference map was calculated, and no peaks above 0.7 e/Å^3 were found. This corresponds to 0.03, 0.05, 0.10, and 0.13 of the heights of iron, phosphorus, oxygen, and carbon atoms, respectively, on a final electron density map.

The final atomic parameters[14] and their standard deviations computed from the least-squares matrix are given in Table I. The important bond lengths are shown in Figures 2 and 3. The important interatomic distances and angles and their calculated standard errors are shown in Tables II and III. Because of the

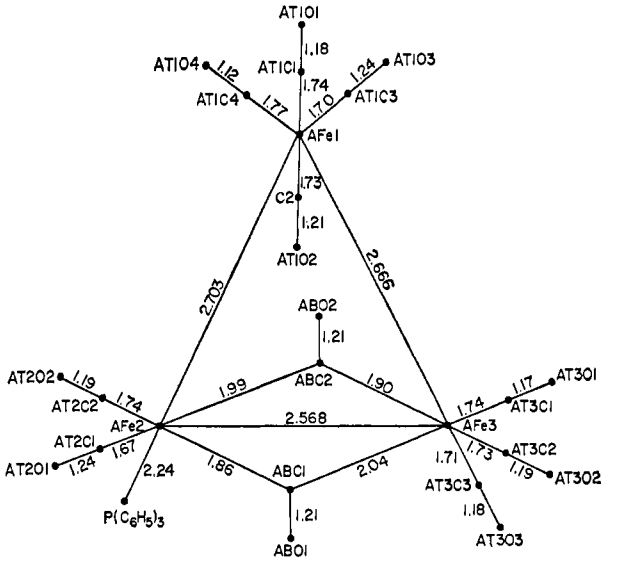

Figure 2. Sketch showing important bond distances in isomer A of $Fe_3(CO)_{11}P(C_6H_5)_3$.

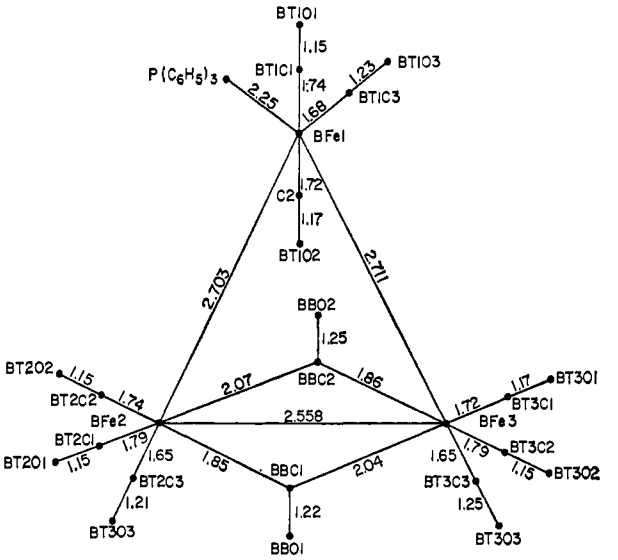

Figure 3. Important bond distances in isomer B.

(12) In addition to programs written in this laboratory for the IBM 7074 and IBM 360-50, other programs used in this work were Johnson's ORTEP to prepare Figures 4 and 5, Busing and Levy's ORFFE to calculate errors, and Busing, Martin, and Levy's ORFLS, modified to allow mixing of isotropic and anisotropic temperature factors. The final cycles of least-squares refinement were performed using Neuman's ORFLS-D. This modification of ORFLS allows rigid body refinement, mixing of temperature factors, and correction for both the real and imaginary parts of anomalous dispersion. All of these options were used.

(13) A list of calculated and observed structure factors based on this refinement has been deposited on Document No. 9979 with the ADI Auxiliary Publications Project, Photoduplication Service, Library of Congress, Washington, D. C. 20540. A copy may be secured by citing the document number and by remitting $1.25 for photoprints, or $1.25 for 35-mm microfilm. Advance payment is required. Make checks or money orders payable to: Chief, Photoduplication Service, Library of Congress.

(14) In all tables, the first letter in the atom designation refers to the molecule in which the atom occurs. Next, for carbon and oxygen atoms, comes the type of group the atom occurs in (terminal, bridging, or ring), followed by the number of the iron atom to which a terminal carbonyl is bonded or the number of the ring. Next comes the chemical symbol for the atom, followed, where necessary, by a number to make the atom designation unique. In the figures, the portion of designation not included can be easily derived.

Table I

Atom	x/a	y/b	z/c	β_{11}[a]	β_{22}	β_{33}	β_{12}	β_{13}	β_{23}
AFe1	0.3958 (2)	0.2132 (5)	0.3506 (2)	8 (1)	48 (6)	17 (1)	−1 (2)	1 (1)	−1 (2)
AFe2	0.4235 (2)	0.4164 (5)	0.3617 (2)	6 (1)	50 (7)	13 (1)	2 (2)	0 (1)	−1 (2)
AFe3	0.4665 (2)	0.2527 (5)	0.3595 (2)	7 (1)	52 (7)	15 (1)	−1 (2)	−1 (1)	1 (2)
BFe1	0.2993 (2)	0.0319 (5)	0.1424 (2)	6 (1)	72 (7)	16 (1)	0 (2)	−1 (1)	−3 (3)
BFe2	0.2362 (2)	0.0979 (6)	0.0944 (2)	8 (1)	100 (8)	17 (2)	8 (2)	−3 (1)	−5 (3)
BFe3	0.2536 (2)	0.1740 (6)	0.1842 (3)	8 (1)	111 (8)	19 (2)	10 (2)	−1 (1)	−14 (3)
AP	0.4507 (3)	0.5789 (9)	0.3705 (4)	5 (1)	46 (13)	9 (2)	1 (3)	−0 (1)	−3 (4)
BP	0.3332 (3)	−0.0769 (10)	0.0957 (4)	7 (1)	72 (14)	12 (2)	2 (3)	−1 (1)	3 (5)

Atom	x/a	y/b	z/c	B	Atom	x/a	y/b	z/c	B
AT1C1	0.399 (1)	0.220 (4)	0.284 (2)	5.4 (12)	AR1C1[b]	0.500	0.573	0.373	3.4 (10)
AT1O1	0.399 (1)	0.218 (2)	0.239 (1)	5.6 (7)	AR1C2	0.518	0.555	0.328	4.0 (10)
AT1C2	0.398 (1)	0.216 (4)	0.417 (2)	6.6 (13)	AR1C3	0.556	0.555	0.331	5.6 (12)
AT1O2	0.396 (1)	0.255 (3)	0.463 (1)	7.8 (9)	AR1C4	0.575	0.572	0.379	4.1 (11)
AT1C3	0.395 (1)	0.075 (4)	0.351 (2)	5.8 (12)	AR1C5	0.557	0.590	0.423	3.7 (10)
AT1O3	0.400 (1)	−0.025 (3)	0.354 (1)	7.2 (9)	AR1C6	0.519	0.591	0.420	3.8 (10)
AT1C4	0.348 (1)	0.227 (4)	0.344 (2)	6.4 (13)	AR2C1	0.442	0.657	0.426	3.4 (10)
AT1O4	0.319 (1)	0.242 (3)	0.344 (1)	8.7 (10)	AR2C2	0.448	0.769	0.425	5.7 (12)
AT2C1	0.390 (1)	0.443 (3)	0.400 (2)	4.6 (11)	AR2C3	0.443	0.833	0.468	8.0 (15)
AT2O1	0.364 (1)	0.462 (1)	0.426 (1)	6.7 (8)	AR2C4	0.431	0.784	0.513	5.6 (12)
AT2C2	0.397 (1)	0.449 (4)	0.306 (2)	4.9 (11)	AR2C5	0.426	0.672	0.514	5.4 (12)
AT2O2	0.379 (1)	0.470 (2)	0.268 (1)	5.7 (8)	AR2C6	0.431	0.608	0.471	5.8 (13)
AT3C1	0.470 (1)	0.155 (4)	0.312 (1)	6.2 (13)	AR3C1	0.438	0.679	0.320	2.7 (9)
AT3O1	0.471 (1)	0.083 (3)	0.282 (1)	6.2 (8)	AR3C2	0.401	0.696	0.311	3.8 (10)
AT3C2	0.472 (1)	0.164 (4)	0.411 (2)	4.6 (11)	AR3C3	0.388	0.770	0.274	4.5 (11)
AT3O2	0.476 (1)	0.104 (3)	0.447 (1)	6.6 (8)	AR3C4	0.412	0.829	0.246	5.1 (11)
AT3C3	0.511 (1)	0.287 (3)	0.362 (1)	3.4 (10)	AR3C5	0.449	0.813	0.255	3.5 (10)
AT3O3	0.543 (1)	0.300 (2)	0.363 (1)	6.0 (8)	AR3C6	0.462	0.738	0.292	4.3 (11)
BT1C1	0.319 (1)	0.150 (4)	1.20 (2)	5.1 (12)	BR1C1	0.326	−0.053	0.026	3.2 (10)
BT1O1	0.337 (1)	0.212 (3)	0.101 (1)	5.9 (8)	BR1C2	0.296	−0.098	−0.001	5.7 (12)
BT1C2	0.272 (1)	−0.071 (4)	0.161 (2)	4.3 (11)	BR1C3	0.289	−0.076	−0.053	4.5 (11)
BT1O2	0.256 (1)	−0.147 (3)	0.175 (1)	5.4 (8)	BR1C4	0.313	−0.009	−0.079	5.8 (12)
BT1C3	0.326 (1)	0.026 (4)	0.197 (2)	5.6 (12)	BR1C5	0.343	0.035	−0.051	6.0 (13)
BT1O3	0.342 (1)	0.024 (2)	0.240 (1)	5.5 (8)	BR1C6	0.350	0.013	0.001	5.5 (12)
BT2C1	0.225 (1)	−0.039 (5)	0.075 (2)	7.0 (14)	BR2C1	0.329	−0.226	0.104	3.1 (10)
BT2O1	0.216 (1)	−0.123 (3)	0.059 (1)	7.9 (9)	BR2C2	0.330	−0.260	0.156	4.4 (11)
BT2C2	0.262 (1)	0.129 (4)	0.044 (2)	5.2 (11)	BR2C3	0.327	−0.371	0.167	5.9 (13)
BT2O2	0.277 (1)	0.157 (2)	0.008 (1)	6.0 (8)	BR2C4	0.324	−0.448	0.127	6.3 (13)
BT2C3	0.198 (1)	0.149 (4)	0.070 (2)	7.3 (14)	BR2C5	0.323	−0.413	0.076	5.3 (12)
BT2O3	0.171 (1)	0.194 (3)	0.051 (1)	9.3 (11)	BR2C6	0.325	−0.302	0.065	5.5 (12)
BT3C1	0.289 (1)	0.252 (4)	0.208 (2)	4.5 (11)	BR3C1	0.382	−0.061	0.108	3.3 (10)
BT3O1	0.314 (1)	0.308 (3)	0.222 (1)	7.7 (9)	BR3C2	0.404	−0.135	0.084	5.6 (12)
BT3C2	0.255 (1)	0.089 (4)	0.240 (2)	4.8 (12)	BR3C3	0.442	−0.126	0.092	5.4 (12)
BT3O2	0.254 (1)	0.034 (3)	0.276 (1)	8.0 (9)	BR3C4	0.457	−0.042	0.123	4.2 (11)
BT3C3	0.221 (1)	0.258 (4)	0.200 (2)	6.8 (14)	BR3C5	0.434	0.132	0.132	5.7 (12)
BT3O3	0.200 (1)	0.325 (3)	0.217 (1)	9.5 (11)	BR3C6	0.397	0.023	0.139	5.0 (11)
ABC1	0.453 (1)	0.358 (4)	0.415 (2)	4.4 (11)	BBC1	0.214 (1)	0.071 (4)	0.155 (2)	4.9 (11)
ABO1	0.466 (1)	0.376 (2)	0.458 (1)	5.2 (7)	BBO1	0.189 (1)	0.024 (3)	0.172 (1)	6.7 (8)
ABC2	0.455 (1)	0.361 (3)	0.309 (2)	4.4 (11)	BBC2	0.255 (1)	0.248 (4)	0.122 (2)	4.4 (11)
ABO2	0.462 (1)	0.382 (2)	0.265 (1)	4.0 (7)	BBO2	0.261 (1)	0.338 (3)	0.102 (1)	6.3 (8)

[a] β's are $\times 10^4$, anisotropic temperature factors are of the form: $\exp(-h^2\beta_{11} - k^2\beta_{22} - l\beta_{33} - 2hk\beta_{12} - 2hl\beta_{13} - 2kl\beta_{23})$. [b] Estimated standard deviations are not given for the ring atoms as they were refined as rigid bodies.

comparatively small number of observations per variable, these results could conceivably be viewed with some distrust. A check on the accuracy of our results is afforded by the positional parameters of the benzene rings which resulted from our first series of refinements. The refined parameters were used to calculate 36 bond distances which were known to be equivalent, thereby giving a very reliable estimate of the errors in this structure determination. The average carbon–carbon bond distance was found to be 1.406 ± 0.007 Å in good agreement with the accepted value, indicating no serious systematic errors in this determination. The standard deviation of an individual measurement of a carbon–carbon bond length as calculated from the distribution of these distances is 0.043 Å. This can be compared to a typical standard deviation of 0.05 Å, calculated for the same type of distance from least squares. This indicates that our error estimates are fairly reliable and that our errors are not underestimated.

Discussion

The molecular structures of the two independent molecules are shown in Figures 4 and 5. Surprisingly, they are structural isomers of one another, an uncommon event, but with some precedence.[15] Also the presence of two isomers is consistent with the bridging C–O absorptions found in the infrared spectra[7] of $Fe_3(CO)_{11}P(C_6H_5)_3$. Two possible explanations which could be advanced to explain the occurrence of the two isomers in each asymmetric unit are that the two forms occur as dimers in solution or that packing is more favorable for the two isomers together than for either separately. The existence of dimers does not appear

(15) I. L. Karle and J. Karle, *Acta Cryst.*, **16**, 969 (1963).

Table II

AFe1–AFe2	2.703 (9)	AFe1–AT1C1	1.74 (5)	AFe1–AT1O1	2.92 (3)	AT1C1–AT1O1	1.18 (4)
AFe1–AFe3	2.666 (8)	AFe1–AT1C2	1.73 (5)	AFe1–AT1O2	2.94 (4)	AT1C2–AT1O2	1.21 (5)
AFe2–AFe3	2.568 (8)	AFe1–AT1C3	1.70 (5)	AFe1–AT1O3	2.93 (4)	AT1C3–AT1O3	1.24 (5)
BFe1–BFe2	2.703 (9)	AFe1–AT1C4	1.77 (5)	AFe1–AT1O4	2.88 (4)	AT1C4–AT1O4	1.12 (5)
BFe1–BFe3	2.711 (9)	AFe2–AT2C1	1.67 (4)	AFe2–AT2O1	2.91 (3)	AT2C1–AT2O1	1.24 (4)
BFe2–BFe3	2.558 (9)	AFe2–AT2C2	1.74 (5)	AFe2–AT2O2	2.93 (3)	AT2C2–AT2O2	1.19 (4)
		AFe3–AT3C1	1.74 (5)	AFe3–AT3O1	2.90 (3)	AT3C1–AT3O1	1.17 (5)
AFe2–AP	2.24 (1)	AFe3–AT3C2	1.73 (5)	AFe3–AT3O2	2.92 (3)	AR3C2–AT3O2	1.19 (4)
BFe1–BP	2.25 (1)	AFe3–AT3C3	1.71 (4)	AFe3–AT3O3	2.88 (3)	AT3C3–AT3O3	1.18 (4)
		BFe1–BT1C1	1.74 (5)	BFe1–BT1O1	2.86 (3)	BT1C1–BT1O1	1.15 (4)
AFe2–ABC1	1.86 (4)	BFe1–BT1C2	1.72 (5)	BFe1–BT1O2	2.88 (3)	BT1C2–BT1O2	1.17 (4)
AFe2–ABC2	1.99 (4)	BFe1–BT1C3	1.68 (5)	BFe1–BT1O3	2.90 (3)	BT1C3–BT1O3	1.23 (4)
AFe3–ABC1	2.04 (4)	BFe2–BT2C1	1.79 (6)	BFe2–BT2O1	2.94 (4)	BT2C1–BT2O1	1.15 (5)
AFe3–ABC2	1.90 (4)	BFe2–BT2C2	1.74 (5)	BFe2–BT2O2	2.89 (3)	BT2C2–BT2O2	1.16 (4)
BFe2–BBC1	1.85 (5)	BFe2–BT2C3	1.65 (5)	BFe2–BT2O3	2.86 (4)	BT2C3–BT2O3	1.21 (5)
BFe2–BBC2	2.07 (4)	BFe3–BT3C1	1.72 (5)	BFe3–BT3O1	2.89 (4)	BT3C1–BT3O1	1.18 (4)
BFe3–BBC1	2.04 (5)	BFe3–BT3C2	1.79 (5)	BFe3–BT3O2	2.94 (4)	BT3C2–BT3O2	1.15 (4)
BFe3–BBC2	1.86 (4)	BFe3–BT3C3	1.65 (6)	BFe3–BT3O3	2.90 (4)	BT3C3–BT3O3	1.25 (5)
AFe2–ABO1	2.93 (3)	BFe2–BBO1	2.91 (3)	ABC1–ABO1	1.21 (4)	AP–	BP–
AFe2–ABO2	3.01 (3)	BFe2–BBO2	3.09 (3)	ABC2–ABO2	1.21 (4)	AR1C1 1.83	BR1C1 1.83
AFe3–ABO1	2.99 (3)	BFe3–BBO1	3.04 (3)	BBC1–BBO1	1.22 (4)	AR2C1 1.78	BR2C1 1.85
AFe3–ABO2	2.93 (3)	BFe3–BBO2	2.96 (3)	BBC2–BBO2	1.25 (4)	AR3C1 1.83	BR3C2 1.83

plausible since the shortest intermolecular distance in the crystal is 3.2 Å. At first glance, the packing argument also appears weak since it seems unlikely that the two isomers should be present in the proper proportions at the proper sites for crystallization to take place. However, the probability of this occurring would be increased by a mechanism suggested by Wojcicki and Pollick,[16] who propose that in solution the bridging bonds are continually being broken and that the bridge is equally likely to re-form between any two of the iron atoms. It is easy to see how the two molecules could be interconverted by this mechanism. This theory is made more palatable by the fact that the bridges are quite asymmetric.

The existence of asymmetric bridging in this structure is unquestionable. Three of the four bridges are asymmetric by more than three standard deviations and the fourth by more than two standard deviations. Since the asymmetry occurs in both isomers, it seems likely that the effect is due to bonding rather than packing considerations and would also occur in the parent compound.[17] A redetermination of the structure of $Fe_3(CO)_{12}$ was reported[18] after this study was begun, but no asymmetry was found in the bridging carbonyls. However, asymmetry in the bridges of $Fe_3(CO)_{12}$ would be hopelessly hidden in the disorder which superposes terminal and bridging carbonyls.[18] Asymmetric bridges might well occur in other previously determined structures but not have been recognized because of the presence of higher pseudo-symmetry.

In general, the arrangement of nonmetal ligands about each iron atom shows surprisingly little distortion from octahedral symmetry. Perhaps the asymmetric bridge is an artifact of the forces which produce this octahedral

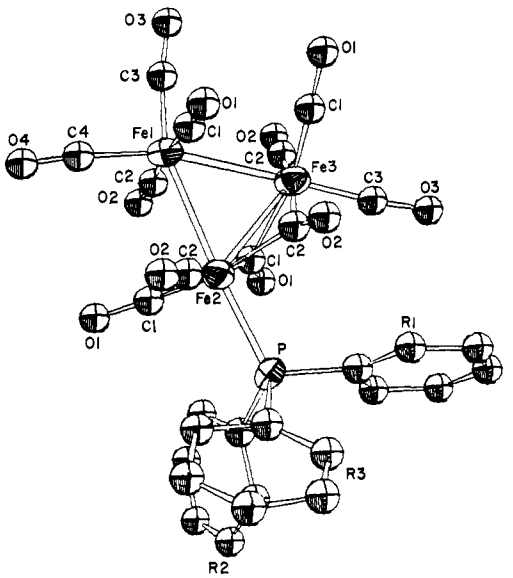

Figure 4. Isomer A of $Fe_3(CO)_{11}P(C_6H_5)_3$ having $P(C_6H_5)_3$ bonded to a bridged iron atom.

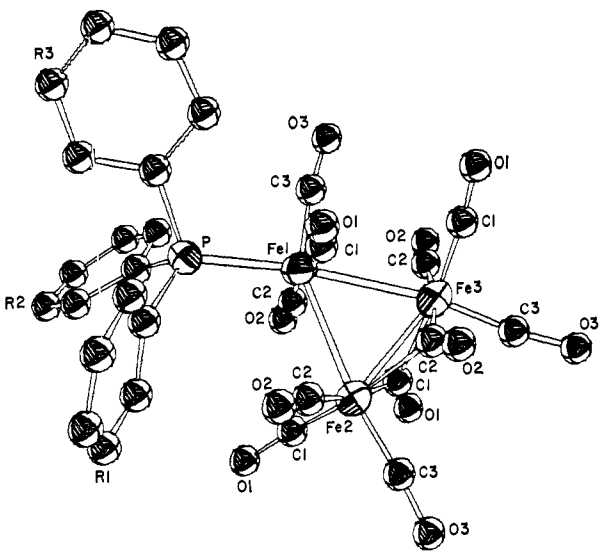

Figure 5. Isomer B of $Fe_3(CO)_{11}P(C_6H_5)_3$ having $P(C_6H_5)_3$ bonded to an unbridged iron atom.

(16) A. Wojcicki and P. J. Pollick, private communication.

(17) D. J. Dahm and R. A. Jacobson, *Chem. Commun.*, 496 (1966).
(18) C. H. Wei and L. F. Dahl, *J. Am. Chem. Soc.*, **88**, 1821 (1966).

Table III

AFe1-AFe2-AFe3	60.7 (2)	AFe1-AT1C1-AT1O1	175 (4)	AT1C1-AFe1-AT1C2	172 (2)
AFe1-AFe3-AFe2	62.1 (2)	AFe1-AT1C2-AT1O2	172 (4)	AT1C1-AFe1-AT1C3	93 (2)
AFe2-AFe1-AFe3	57.1 (2)	AFe1-AT1C3-AT1O3	171 (4)	AT1C1-AFe1-AT1C4	92 (2)
BFe1-BFe2-BFe3	62.0 (3)	AFe1-AT1C4-AT1O4	174 (5)	AT1C2-AFe1-AT1C3	91 (2)
BFe1-BFe3-BFe2	61.6 (3)	AFe2-AT2C1-AT2O1	176 (4)	AT1C2-AFe1-AT1C4	95 (2)
BFe2-BFe1-BFe3	56.4 (2)	AFe2-AT2C2-AT2O2	179 (4)	AT1C3-AFe1-AT1C4	95 (2)
		AFe3-AT3C1-AT3O1	175 (4)	AT2C1-AFe2-AT2C2	93 (2)
AFe2-ABC1-AFe3	82 (2)	AFe3-AT3C2-AT3O2	179 (4)	AT2C1-AFe2-ABC1	92 (2)
AFe2-ABC2-AFe3	83 (2)	AFe3-AT3C3-AT3O3	173 (4)	AT2C1-AFe2-ABC2	167 (2)
BFe2-BBC1-BFe3	82 (2)	BFe1-BT1C1-BT1O1	166 (4)	AT2C2-AFe2-ABC1	170 (2)
BFe2-BBC2-BFe3	81 (2)	BFe1-BT1C2-BT1O2	174 (4)	AT2C2-AFe2-ABC2	80 (2)
		BFe1-BT1C3-BT1O3	172 (4)	ABC1-AFe2-ABC2	93 (2)
AFe2-ABC1-ABO1	144 (4)	BFe2-BT2C1-BT2O1	173 (5)	AT3C1-AFe3-AT3C2	96 (2)
AFe2-ABC2-ABO2	139 (3)	BFe2-BT2C2-BT2O2	173 (4)	AT3C1-AFe3-AT3C3	95 (2)
AFe3-ABC1-ABO1	132 (3)	BFe2-BT2C3-BR2O3	175 (5)	AT3C1-AFe3-ABC1	169 (2)
AFe3-ABC2-ABO2	139 (3)	BFe3-BTC31-BT3O1	177 (4)	AT3C1-AFe3-ABC2	91 (2)
BFe2-BBC1-BBO1	142 (4)	BFe3-BT3C2-BT3O2	177 (4)	AT3C2-AFe3-AT3C3	94 (2)
BFe2-BBC2-BBO2	135 (3)	BFe3-BT3C3-BT3O3	172 (4)	AT3C2-AFe3-ABC1	82 (2)
BFe3-BBC1-BBO1	136 (4)			AT3C2-AFe3-ABC2	171 (2)
BFe3-BBC2-BBO2	144 (3)	AFe2-AP-AP1C1	115	AT3C3-AFe3-ABC1	96 (2)
		AFe2-AP-AR2C1	117	AT3C3-AFe3-ABC2	91 (2)
AP-AFe2-ABC1	91 (1)	AFe2-AP-AR3C1	116	ABC1-AFe3-ABC2	90 (2)
AP-AFe2-ABC2	95 (1)	BFe1-BP-BR1C1	113	BT1C1-BFe1-BT1C2	169 (2)
AP-AFe2-AT2C1	96 (1)	BFe1-BP-BR2C1	117	BT1C1-BFe1-BT1C3	95 (2)
AP-AFe2-AT2C2	96 (1)	BFe1-BP-BR3C1	115	BT1C2-BFe1-BT1C3	93 (2)
BP-BFe1-BT1C1	92 (1)			BT2C1-BFe2-BT2C2	97 (2)
BP-BFe1-BT1C2	95 (1)	AFe1-AFe2-AT2C1	87 (1)	BT2C1-BFe2-BT2C3	94 (2)
BP-BFe1-BT1C3	96 (2)	AFe1-AFe2-AT2C2	86 (1)	BT2C1-BFe2-BBC1	88 (2)
		AFe1-AFe3-AT3C1	86 (1)	BT2C1-BFe2-BBC2	173 (2)
AFe1-AFe2-AP	175.5 (3)	AFe1-AFe3-AT3C2	91 (1)	BT2C2-BFe2-BT2C3	98 (2)
AFe3-AFe2-AP	114.8 (4)	AFe1-AFe3-AT3C3	175 (1)	BT2C2-BFe2-BBC1	171 (2)
BFe2-BFe1-BP	115.3 (4)	AFe2-AFe1-AT1C1	91 (2)	BT2C2-BFe2-BBC2	83 (2)
BFe3-BFe1-BP	170.9 (4)	AFe2-AFe1-AT1C2	83 (2)	BT2C3-BFe2-BBC1	89 (2)
		AFe2-AFe1-AT1C3	158 (2)	BT2C3-BFe2-BBC2	93 (2)
AFe1-AFe3-ABC1	86 (1)	AFe2-AFe1-AT1C4	107 (2)	BT3C1-BFe3-BT3C2	93 (2)
AFe1-AFe2-ABC2	81 (1)	AFe2-AFe3-AT3C1	129 (2)	BT3C1-BFe3-BT3C3	97 (2)
AFe1-AFe3-ABC1	83 (1)	AFe2-AFe3-AT3C2	121 (1)	BT3C1-BFe3-BBC1	175 (2)
AFe1-AFe3-ABC2	84 (1)	AFe2-AFe3-AT3C3	114 (1)	BT3C1-BFe3-BBC2	89 (2)
AFe2-AFe3-ABC1	46 (1)	AFe3-AFe1-AT1C1	87 (1)	BT3C2-BFe3-BT3C3	98 (2)
AFe2-AFe3-ABC2	50 (1)	AFe3-AFe1-AT1C2	86 (2)	BT3C2-BFe3-BBC1	86 (2)
AFe3-AFe2-ABC1	52 (1)	AFe3-AFe1-AT1C3	101 (2)	BT3C2-BFe3-BBC2	173 (2)
AFe3-AFe2-ABC2	47 (1)	AFe3-AFe1-AT1C4	164 (2)	BT3C3-BFe3-BBC1	88 (2)
BFe1-BFe2-BBC1	88 (1)	AFe3-AFe2-AT2C1	131 (1)	BT3C3-BFe3-BBC2	88 (2)
BFe1-BFe2-BBC2	81 (1)	AFe3-AFe2-AT2C2	118 (1)	BBC1-BFe2-BBC2	91 (2)
BFe1-BFe3-BBC1	85 (1)	BFe1-BFe2-BTC23	174 (2)	BBC1-BFe3-BBC2	92 (2)
BFe2-BFe3-BBC2	85 (1)	BFe1-BFe3-BT3C3	170 (2)		
BFe2-BFe3-BBC1	46 (1)	BFe2-BFe1-BT1C3	148 (2)	BFe1-BFe2-BT2C1	92 (2)
BFe2-BFe3-BBC2	53 (1)	BFe3-BFe1-BT1C3	92 (2)	BFe1-BFe2-BT2C2	85 (1)
BFe3-BFe2-BBC1	52 (1)	BFe2-BFe1-BT1C1	88 (1)	BFe1-BFe3-BT3C1	91 (1)
BFe3-BFe2-BBC2	46 (1)	BFe3-BFe1-BT1C1	84 (1)	BFe3-BFe2-BT2C1	129 (2)
		BFe3-BFe1-BT1C2	88 (1)	BFe3-BFe2-BT2C2	120 (2)
BFe2-BFe3-BT3C1	132 (1)	BFe2-BFe3-BT3C3	108 (2)	BFe3-BF32-BT2C3	112 (2)
BFe2-BFe3-BT3C2	121 (1)	BFe2-BFe1-BT1C2	81 (1)	BFe1-BFe3-BT3C2	88 (1)

arrangement. If both bridged iron atoms and bridging carbonyls were in the same plane, symmetric bridging would appear reasonable. However, each bridged iron atom is turned so that the apex of an octahedron is pointed within 6° of the unbridged iron atom. To retain symmetric bridging in this situation, one or more of the following must occur: the iron-bridging carbon distances must be lengthened considerably, the iron–iron distance must be shortened increasing the repulsion of the bridged iron atoms, or the bridging carbonyls must be drawn from their positions toward each other increasing their mutual repulsion. In an asymmetric bridge, the repulsions between bridging carbonyls are alleviated, though the carbon atoms are still only 2.8 Å apart, and one iron-bridging carbon bond can be of essentially normal length. The symmetric bridge[19] in $HFe_3(CO)_{11}^-$ can be explained by the lesser spatial requirements of the bridging hydride (H^-) in comparison to a carbonyl group.

A comparison of the two isomers shows considerable variation in unbridged iron–iron bonds. The distance between two iron atoms, neither of which is bonded to a phosphorus atom, is similar to that found for unsubstituted $Fe_3(CO)_{12}$ (2.67 *vs.* 2.68 Å) while the iron–iron distances involving the iron atoms which are bonded to a phosphorus atom are significantly longer. As described below, this lengthening might be due to increased population in antibonding orbitals. The bridged iron–iron bond is kept from lengthening extensively by the carbonyl bridges.

It might be expected that iron–carbon bonds opposite the longer bridging carbonyl bonds would be shorter than those opposite the shorter bridging bonds. Such variation could result from a weakening of the π bond (and possibly the σ bond also) in the lengthened bond

(19) L. F. Dahl and J. F. Blount, submitted for publication.

and a consequent increase in the strength of the opposite bond, thereby causing a shortening. While it is impossible on the basis of statistics to say that the iron–carbon and carbon–oxygen distances in the terminal bonds are not all equivalent, there does seem to be a shortening in the iron–carbon bonds opposite the iron–iron bonds. Using the same arguments, the latter effect should occur and be larger than the former because there would be little π character in the iron–iron bond. One would also expect lengthened carbon–oxygen distances in those cases where shortening of the iron–carbon distance has taken place. This effect appears to be present although admittedly it could be magnified by errors in carbon positions.

The iron–carbon bond lengths around the iron atoms which are bonded to a phosphorus atom (av 1.71 Å) appear in general to be somewhat shorter than those around the other iron atoms (av 1.72 Å). If real, this could result from the inability of a $P(C_6H_5)_3$ group to compete with carbonyls as π-electron acceptors as effectively as the carbonyl which it replaces. Such shortening has previously been evidenced by a lower C–O stretching frequency for unsubstituted metal carbonyls than for the corresponding monosubstituted triphenylphosphine derivative.[20] Angelici has proposed[21] that there is a transfer of electron density from the metal–phosphorus σ bond to the metal–carbon π bond. Such transfer would also cause a decrease in metal–carbon bond length.

Several of the iron–carbon–oxygen angles in the terminal carbonyls vary considerably from 180°. This is frequently observed in lower symmetry systems and can be attributed to bonding as well as steric and packing considerations.[22]

The temperature factors of the carbonyl atoms are somewhat large as might be expected from the rapid fall of intensity. It is not surprising that the oxygen atoms at the end of the carbonyls have larger temperature factors than the carbon atoms to which they are bonded. The ring carbon atoms have considerably smaller temperature factors, and in every ring the carbon atom bonded to the phosphorus has a smaller temperature factor than the other atoms in the ring.

In a molecule of this complexity it is indeed hard to distinguish between causes of primary effects and secondary effects, but the over-all trends found in the structure do not seem unexpected in the light of present understanding.

In view of the widespread differences of opinion as to the interpretation of experimental results for the structure of $Fe_3(CO)_{12}$, it would be interesting to see if the most nearly correct structure could have been picked from those shown in Figure 1 from theoretical arguments. The treatment presented here by no means constitutes a rigorous proof and of course was aided by the knowledge of the structure of $Fe_3(CO)_{11}P(C_6H_5)_3$.

We will assume that in the correct structure the bonding will be such that all iron atoms will attain the krypton configuration, and that no iron atom will be bonded to more than seven other atoms. The first assumption is known to hold true for the vast majority of metal carbonyls,[23] and the second seems reasonable for an atom the size of iron.

In the linear arrangement (Figure 1c), the center iron atom does not attain a filled shell with or without bonds being formed between iron atoms. If iron–iron bonds are formed, the center iron atom has eight bonds; if not, none of the iron atoms attains a filled shell. In fact, no linear arrangement which satisfies both assumptions is readily apparent.

A triangular arrangement with six bridging carbonyls (Figure 1d) seems less likely than a linear arrangement on the basis of valence-bond and spatial arguments. Three iron–iron bonds are necessary for the iron atoms to fill their shells, but such bonding gives each iron atom eight bonds.

On the basis of the above assumptions, triangular arrangements with either zero or two bridging carbonyls seem equally likely. A molecular orbital treatment was carried out to see if one of these could be ruled out on the basis of energy requirements. The method used was very similar to one described for benzene.[24] Each iron–carbon bond was assumed to use a d^2sp^3 orbital from an iron atom and only the remaining d^2sp^3 and d orbitals from the iron atoms were used to form the molecular orbitals which can be thought of as holding the iron atoms together. The values of the resonance integral representing interactions between pairs of atomic orbitals were assigned symbols and ranked qualitatively on the basis of examination of a ball and stick model.

The molecule with no bridging carbonyls (Figure 1b) would have D_{3h} symmetry. Of the total 48 bonding electrons and 27 iron orbitals, the iron–carbon σ bonds would use 24 electrons and 12 iron orbitals, leaving 24 electrons to be placed in 15 molecular orbitals. Our calculations showed that seven of these orbitals would be bonding and eight antibonding.

The molecule with two bridging carbonyls was treated as having C_{2v} symmetry. The iron–carbon bonds take up 28 electrons and use five orbitals each from two iron atoms and four from the other. This leaves 20 electrons to be placed in 13 molecular orbitals. In setting up the calculations, it was apparent that two types of interactions, where atomic orbitals from two iron atoms were nearly collinear, would give a much larger value for the resonance integral than other interactions where atomic orbitals formed angles considerably less than 180°. Initially all of the small resonance integrals were assumed to be zero. This model gave three bonding orbitals, three very antibonding orbitals, and seven nonbonding orbitals. Thus this model would appear to be energetically feasible, inasmuch as none of 20 electrons needs be put in antibonding orbitals.

While the symmetry of the bridged structure does seem more favorable, one might wonder why the structures of $Ru_3(CO)_{12}$ and $Os_3(CO)_{12}$ are not also bridged on this basis.[25,26] It seems reasonable that bridging in those cases would necessitate a closeness of approach of the larger ruthenium and osmium atoms which would be prohibitive.[26] Indeed, since the bridges in Fe_3-

(20) F. A. Cotton and G. Wilkinson, "Advanced Inorganic Chemistry," Interscience Publishers, New York, N. Y., 1962.
(21) R. J. Angelici and M. D. Malone, *Inorg. Chem.*, **6**, 1731 (1967).
(22) S. F. A. Kettle, *ibid.*, **4**, 1661 (1965).
(23) R. E. Rundle, *Surv. Progr. Chem.*, **1**, 81 (1963).
(24) H. Eyring, J. Walter, and G. Kimball, "Quantum Chemistry," John Wiley and Sons, Inc., New York, N. Y., 1954, pp 256–257.
(25) E. R. Corey and L. F. Dahl, *Inorg. Chem.*, **1**, 521 (1962).
(26) E. R. Corey and L. F. Dahl, *J. Am. Chem. Soc.*, **83**, 2203 (1961).

$(CO)_{12}$ are asymmetric, the feasibility of this arrangement in the case of iron is probably marginal.

It should be noted that in the above calculations it has been assumed that all iron–carbon bonds are σ bonds with a bond order of 1, and all π bonding has been neglected. Also the interactions which were neglected could no doubt be used to break the degeneracy of the nonbonding orbitals. Such crude approximations might suffice for checking the feasibility of a certain structure, but we recognize their limited application for a detailed description of electronic arrangement.

A treatment of the correct structure which did not neglect most of the small interactions was also carried out. In this case the energies of the orbitals which had been bonding and antibonding before were unchanged, but the seven nonbonding orbitals became three bonding and four weakly antibonding orbitals.

There are several p orbitals on carbon atoms which have the proper symmetry to π-bond with the iron atoms. Therefore, it seems reasonable that much of the electron density in these iron–iron antibonding orbitals will be transferred to iron–carbon π bonds, thereby increasing the net strength of the iron–iron bonds. If one then replaces a carbonyl with a lesser π-bonding triphenylphosphine, these antibonding orbitals should be given additional electron density. This would weaken the iron–iron bonds and result in the longer iron–iron distances noted in this structure determination.

Acknowledgment. We thank Mr. Edwin Siefert for preparing the single crystals used in this study and Professor Robert J. Angelici for calling the existence of this compound to our attention and for his helpful discussions concerning its structure.

The Electronic Structure and Donor Properties of Cyanamides[1]

H. Fred Henneike and Russell S. Drago

Contribution from the W. A. Noyes Laboratory, University of Illinois, Urbana, Illinois. *Received February 23, 1968*

Abstract: Extended Hückel calculations have been carried out on dimethylcyanamide [$(CH_3)_2NCN$], cyanamide (H_2NCN), and acetonitrile. The minimum energy geometry is calculated for the nonplanar structure in agreement with the results from microwave studies. Various molecular properties are calculated in an attempt to understand why dimethylcyanamide is a better donor than acetonitrile toward a whole series of Lewis acids. Calculations on the BF_3 adducts of these donors are most illuminating. By examining the energies of the empty π orbitals of acetonitrile and dimethylcyanamide, we gain support for our previous qualitative rationalization of the fact that, in contrast to their donor properties, the spectrochemical parameter *Dq* toward nickel(II) for acetonitrile is larger than that for dimethylcyanamide.

Structural investigations on the cyanamides have been confined almost exclusively to cyanamide itself. A crystal structure study of cyanamide[2,3] yielded the paremeters below.

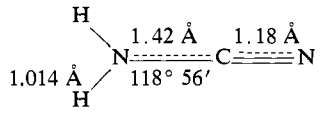

HNH angle (not shown) = 106° 47′

All of the parameters except possibly the N–H distance are at serious variance with the results of microwave studies on cyanamide in the vapor phase. Tyler, *et al.*,[4] find the total N–C–N distance to be 2.507 ± 0.003 Å and the HNH angle equal to 120 ± 1°. The authors present evidence for the bond lengths $r_{C\equiv N}$ = 1.16 ± 0.01 Å and $r_{N=C}$ = 1.35 ± 0.01 Å. A more complete analysis[5,6] substantiated the microwave findings and further suggested that superimposed on the parabolic potential function of the NH_2 out-of-plane bending vibration there is a small symmetric hump centered at the planar position causing cyanamide to have a nonplanar (C_s) equilibrium configuration. Fletcher and Brown[7] were able to fit all their observations of infrared and Raman bands through use of a Manning[8] potential for this vibration with a barrier height of 660 ± 20 cm^{-1} and an equilibrium out-of-plane bending angle of approximately 20°. It does not seem possible to reconcile the mutually longer bond lengths of the crystal-structure study with these results even by invoking various modes of hydrogen bonding in the crystal. It seems likely that the microwave data are the more accurate. Other authors[9–11]

(1) Abstracted in part from the Ph.D. thesis of H. F. Henneike, University of Illinois, 1967. Address inquiries to Chemistry Department, University of Minnesota, Minneapolis, Minn.
(2) C. L. Christ, *Acta Cryst.*, 4, 77 (1951).
(3) "Cyanamide," American Cyanamid Co., Applied and Process Chemicals Department, 1963, p 13.
(4) J. K. Tyler, L. F. Thomas, and J. Sheridan, *Proc. Chem. Soc.*, 155 (1959).
(5) D. R. Lide, Jr., *J. Mol. Spectry.*, 8, 142 (1962).
(6) D. J. Millen, G. Topping, and D. R. Lide, Jr., *ibid.*, 8, 153 (1962).
(7) W. H. Fletcher and F. B. Brown, *J. Chem. Phys.*, 39, 2478 (1963).
(8) M. F. Manning, *ibid.*, 3, 136 (1935).